The Role of Hydrophobic Chains in Self-Assembly at Electrified Interfaces: Observation of Potential-Induced Transformations of Two-Dimensional Crystals of Hexadecane by In-situ Sca...

ARTICLE *in* THE JOURNAL OF PHYSICAL CHEMISTRY B · OCTOBER 2002

Impact Factor: 3.3 · DOI: 10.1021/jp021106e

3 AUTHORS:

Yufan He
Bowling Green State University
38 PUBLICATIONS **685** CITATIONS
SEE PROFILE

Tao Ye
University of California, Merced
34 PUBLICATIONS **973** CITATIONS
SEE PROFILE

Eric Borguet
Temple University
143 PUBLICATIONS **2,654** CITATIONS
SEE PROFILE

The Role of Hydrophobic Chains in Self-Assembly at Electrified Interfaces: Observation of Potential-Induced Transformations of Two-Dimensional Crystals of Hexadecane by In-situ Scanning Tunneling Microscopy

Yufan He, Tao Ye, and Eric Borguet*

Department of Chemistry and Surface Science Center, University of Pittsburgh, Pittsburgh, Pennsylvania 15260

Received: May 2, 2002; In Final Form: August 8, 2002

Insoluble alkanes have been observed by electrochemical scanning tunneling microscopy (STM) to form ordered monolayers at the Au(111)/0.1 M $HClO_4$ solution interface. Hexadecane molecules self-assemble into ordered layers that are stable over the potential range from 0.15 V_{SCE} to 0.55 V_{SCE}, on both reconstructed and unreconstructed Au(111) surfaces under electrochemical control. The hexadecane molecules appear as 2.2 nm long and 0.45 nm wide rods, suggesting an extended conformation. STM images show that a reversible order−disorder transition can be induced by moving the electrode potential positive or negative of the stable potential region (0.15 V_{SCE} to 0.55 V_{SCE}). The hexadecane molecules aggregate immediately after lifting of the surface reconstruction by a positive potential step to 0.65 V_{SCE}. Reversible disappearance of the ordered alkane structure is also observed when the potential is stepped below 0.15 V_{SCE}. The molecules resume an ordered lamellar structure upon return of the substrate to the stable potential region. A critical role for the aqueous solvent in inducing the phase transition is proposed.

1. Introduction

1.1. Role of Hydrophobic Tails in the Structure of Amphiphilic Monolayers. Adsorbed organic thin films, often residing at charged interfaces, afford opportunities in molecular level engineering of surfaces for applications ranging from sensors[1] and corrosion protection[2] to biomembrane functions and colloidal systems.[3,4] The interfacial charge may affect the structure and properties of thin films. Understanding and controlling the charge-dependent structures and properties is important for preparing and controlling the properties of organic thin films on electrode surfaces for various applications.[5−8]

Most organic thin films at charged interfaces are composed of amphiphilic molecules consisting of hydrophobic tails and hydrophilic headgroups, whose potential-dependent structure is a result of complex interactions between the hydrophobic tails, the headgroups, the electrolyte, and the substrate. Changes in molecular orientation and packing,[9,10] desorption,[9] and formation of surface aggregates such as micelles[11,12] may occur in adsorbed amphiphilic molecules upon modulation of the surface charge. The competitive adsorption of electrolyte and hydrocarbon chains on electrodes is recognized as a dominant factor in the structure of weakly adsorbed amphiphilic molecules.[9] Near the potential of zero charge (pzc) in aqueous environments, hydrophobic repulsion orients the hydrophobic hydrocarbon chains of physisorbed amphiphilic molecules toward the metal surface while the hydrophilic headgroups point toward the aqueous electrolyte.[9] However, at sufficiently high surface charge density, hydrophobic hydrocarbon chains on electrode surfaces are displaced by the electrolyte, resulting in a change in orientation or desorption.[9] Even for self-assembled monolayers, formed by molecules with headgroups binding strongly to the substrate through chemisorption, in which one would expect diminishing influence from the weakly interacting tails, the hydrophobic tails remain critical in determining the formation and stability of the monolayers at electrified interfaces. For example, increasing the length of the alkyl chains has been found to improve the stability at negative potential of alkanethiol monolayers.[6,7,13] Hatchett et al. found that the adsorption free energies of *n*-alkanethiolates under aqueous solution increased by 1 kcal/mol with each additional methylene unit in the chain.[7] The increased stability has been attributed to increasing hydrophobic interactions under aqueous solution, improved screening of ions, and the increased stabilization by van der Waals interactions between the chains.[6,7,13] It was proposed that for alkanethiols with chain length longer than 10 carbons, the contribution from alkyl chains to the adsorption energy (10−20 kcal/mol) is comparable to that from the chemisorbed sulfur headgroups (20−30 kcal/mol).[7]

1.2. Studies of Alkanes at Electrified Interfaces. 2D hydrophobic phases, such as normal alkanes confined at electrified interfaces, represent an interesting model system to understand the role of hydrophobic tails of amphiphilic molecules. Although the hydrophobic tails are frequently invoked to explain the structure and properties of amphiphilic molecules at solid−liquid interfaces, there has been little experimental effort to separately study the structure and dynamics of completely hydrophobic molecules, such as alkanes, at these interfaces. Wu et al. studied the penetration of ions across hydrophobic phases in the presence of electric fields by depositing hydronium ions on alkane films on Pt(111).[14] The activation barrier for the ion penetration through 3-methylpentane was determined to be 38 kJ/mol.[14] Ivosevic et al. studied the spreading of hydrocarbon droplets at the dropping mercury electrode (DME).[15] It was found that various hydrocarbons could spread on the DME within a potential range near the pzc. Longer alkanes spread more readily than shorter ones, presumably due

* Corresponding author: E-mail: borguet@pitt.edu.

10.1021/jp021106e CCC: $22.00
Published on Web 10/08/2002

to more molecule−substrate interactions. However, the existing studies are mostly limited to the thermodynamic description of the interfaces, e.g., measurement of interfacial tension. What is largely unexplored and of particular interest is the surface charge driven microscopic structure and dynamics that correspond to the spreading or aggregation of alkanes on metal electrodes. In this respect, STM, capable of tracking the evolution of individual molecules, provides a particularly powerful approach to tackle this complex problem.

1.3. Summary of Previous Investigations of the Structure of Alkanes on Au Surfaces. To understand the largely unexplored alkane thin film structures at electrified interfaces, it is instructive to review existing studies of alkanes adsorbed on metal surfaces in UHV or under nonpolar solvents. Such studies can elucidate the role of intermolecular and molecule−substrate interactions, which should be relevant in determining the structures of alkanes at electrified interfaces despite the additional complexity arising from the electric field dependent electrolyte-substrate and electrolyte−adsorbate interactions.

The physisorption of alkanes on single-crystal metal surfaces has served as a model system. For long-chain *n*-alkanes (>C6), the physisorption energy on Au increases linearly with the chain length by 6.2 ± 0.2 kJ/mol per additional methylene unit.[16] Solvation force measurements, temperature programmed desorption, molecular dynamics, and Monte Carlo simulations suggest the formation of alkane layered structures near solid surfaces due to adsorbate−substrate interactions.[17−19] Reflection absorption infrared spectroscopy[20−22] and low energy electron diffraction (LEED)[23] reveal that adsorbed linear alkanes adopt an all-trans conformation in ordered layers, with the zigzag plane of the molecules aligning parallel to the substrate surface.

Scanning tunneling microscopy (STM) studies have provided unprecedented structural details about the physisorbed alkanes, mainly on graphite surfaces.[24] However, STM investigations of alkanes adsorbed on metal surfaces have appeared only recently.[25−31] It was found that the structure of the 2D alkane crystals depends on the substrate crystallography.[27,28] The long molecular axis of the alkane molecules was preferentially oriented along the $[01\bar{1}]$ or $[1\bar{1}0]$ direction of the substrate, i.e., at 30° with respect to the stripes of the reconstruction on Au(111).[27,28] Thus, a relatively complete picture of alkane adsorption has emerged in UHV and under nonpolar solvents, enabling us to address the additional complexities that the aqueous electrolyte and electric fields can introduce.

1.4. Summary of the Present Work. We report a high-resolution STM investigation of potential dependent structures of hexadecane on Au(111) under an electrochemical environment. The experiments reported here afford a molecular level understanding of the structure of the hydrophobic phase at electrified interfaces. A variety of charge-dependent structures of the hydrophobic phase at the interfaces, including the surface charge induced order−disorder phase transitions as well as the formation of nanometer-sized alkane aggregates, are demonstrated. Consideration of the role of competitive adsorption between the hydrophobic alkane molecules and aqueous electrolyte enables the structures to be rationalized. The observation of rich dynamic behavior, such as the propagation of domains, and flipping of molecular orientations offer insight into the role of intermolecular interactions in the dynamics of 2D phase transitions. In addition, the observation of 2D hexadecane crystal on unreconstructed Au(111) under electrochemical environment, which could not be observed under nonpolar solvent,[28] suggests that the aqueous electrolyte may promote the ordering of the hydrophobic thin film. It is hoped that such molecular level understanding of the hydrophobic phase under electrolyte will contribute to the elucidation of the structure and dynamics of amphiphilic molecules at electrified interfaces.

2. Experimental Section

2.1. Preparation of Samples. The Au(111) single-crystal substrate, a disk 1 cm in diameter and 2 mm thick (Monocrystals Co., Ohio), was cleaned by immersion in hot piranha solution (1:3 H_2O_2 (reagent grade, J. T. Baker) and H_2SO_4 (reagent grade, J. T. Baker)) for 1 h, and immersion in hot HNO_3 (reagent grade, EM Science) for 30 min. **(Caution! The piranha solution is a very strong oxidizing reagent and extremely dangerous to handle. Protective equipment including gloves and goggles should be used at all times.)** After each step the sample was rinsed by ultrasonication in ultrapure water (>18 MΩ·cm). The crystal was hydrogen flame annealed, and allowed to cool to room temperature in air. A drop of hexadecane (Acros, 99%) was placed on the surface and rinsed with decane, then allowed to dry in air. The crystal was transferred to the STM electrochemical cell and immersed under potential control (0.25 V_{SCE}) in 0.1 M $HClO_4$ (Optima grade, Fisher Scientific) solution.[32] A Teflon STM cell ensured that only the (111) facet was exposed to electrolyte. The substrate was occasionally electropolished at 3 V potential in 1 M H_2SO_4 solution.[33] All electrode potentials are quoted relative to the SCE potential.

2.2. STM Experiment. STM images were obtained with a PicoScan STM system (Molecular Imaging). A bipotentiostat (Molecular Imaging) was used to control the sample and tip potential independently. The electrochemical cell was made of Teflon. A silver wire and a platinum wire were used as a quasi-reference electrode and counter electrode, respectively. All cell components were chemically cleaned in the same way as the crystal. STM tips were prepared by electrochemically etching 0.25 mm diameter tungsten wires using 10 V AC, in 3 M KOH solution. Tips, coated with paraffin wax, yielded less than 10 pA Faradic current. All the STM images were obtained under constant current mode at 1.1 nA. The tip potential was kept at $0V_{SCE}$, so that the tip−sample bias tracked the sample potential in the range from 0.05 to 0.65 V. Additional details of the STM experiment can be found elsewhere.[32]

3. Results

3.1. Structure of Hexadecane Monolayers on Reconstructed Au(111) Surface. STM images of hexadecane at the Au(111)/0.1M $HClO_4$ solution interface at 0.25 V_{SCE} (Figure 1) show a molecular row structure crossing the substrate double stripes. The underlying double stripe structure, 0.1 to 0.2 Å high, is due to the reconstruction of the Au(111) surface[34,35] and is clearly visible even in the presence of adsorbed molecules. The Au(111) surface has two stable phases; the unreconstructed (1 × 1), consistent with a bulk termination, and the reconstructed ($22 \times \sqrt{3}$), where the surface atoms are slightly compressed in [110] directions.[34] In an electrochemical environment, a transition between the two phases can be induced by changing the electrode potential.[35] The reconstructed surface is stable at potentials when the surface has a negative excess charge. It is now well established that the reconstructed Au(111)−($22 \times \sqrt{3}$) surface transforms to the Au(111)−(1 × 1) phase at potentials above ~440 mV_{SCE}, and that the reverse transition occurs for potentials below ~220 mV_{SCE} in $HClO_4$ solution.[36] The density of the reconstructed phase is estimated to be about 4.5% higher than the unreconstructed phase.[35] The periodicity of the double stripes of the alkane-covered reconstruction is about 63 Å, nearly identical to that observed on a bare Au(111) under electrolyte.[35]

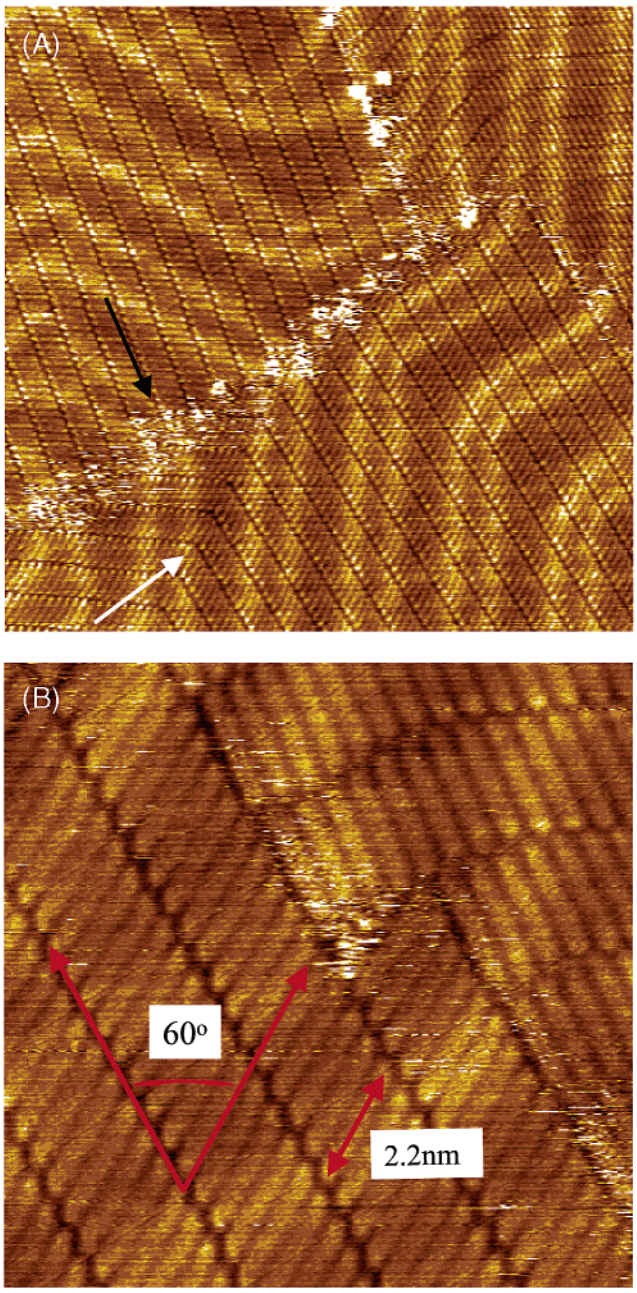

Figure 1. Hexadecane on reconstructed Au(111)/0.1 M $HClO_4$ interface at 0.25 V_{SCE}. Molecules adopt extended conformation as 2.2 nm long and 0.45 nm wide rods parallel to the surface. The molecular axes cross the rows at about 60°. The domain boundaries of the molecular rows are pinned by the domain structure of the reconstruction stripes of the gold surface, as indicated by a black arrow. Scan area (A) 42 × 42 nm^2; (B) 10 × 10 nm^2.

A high-resolution image, Figure 1B, shows that the molecular rows consist of rods 2.2 nm in length, separated by 0.45 ± 0.02 nm, measured perpendicular to the molecular axis. The molecular axes cross the rows at about 60°. The 2.2 nm length is in agreement with the calculated length of hexadecane in an all-trans conformation,[37] suggesting that the rods in the STM images correspond to individual hexadecane molecules in an all-trans conformation with the molecular axis parallel to the surface plane. The clear observation of the double stripe substrate structure in the present work indicates that adsorption of alkanes does not lift the Au(111) reconstruction.

The molecular layers adopt a well-defined structure with respect to the underlying substrate. The molecular axis was preferentially oriented at 30° with respect to the stripes of the gold reconstruction. This result is in agreement with the reported STM result for hexadecane adsorbed on Au(111) under neat hexadecane in air, where the preferential orientation of the molecular axis is along nearest neighbor (NN) direction (the $[01\bar{1}]$ or $[1\bar{1}0]$ direction of the substrate), i.e., at 30° with respect to the stripes of gold reconstruction.[25,26,28] A consequence of this arrangement is the existence of two equivalent directions of the molecular rows, at +30° and −30° with respect to the double stripes of the Au(111) reconstruction.

The influence of the Au(111) surface reconstruction on the structure of the 2D alkane crystal is apparent as shown in Figure 1A and B. Noisy domain boundaries, indicated by a black arrow in Figure 1A, are formed between molecular rows with different molecular axis orientations. The noise suggests mobility of molecules at the edges of the domains. Interestingly, the domain boundaries of the molecular rows are located at the substrate reconstruction domain boundaries, i.e., the elbows in the double rows of the herringbone structure. Within the same domain, even if the molecular rows change direction, the molecular axis direction does not change (Figure 1A as indicated by a white arrow). These results are in good agreement with those reported by Uosaki et al. under nonpolar solvent.[25−27]

3.2. Potential-Induced Transformation of 2D Hexadecane Crystals on Au(111). *3.2.1. Order−Disorder Transitions at Potentials Positive of the pzc.* To study the effect of the substrate potential, and the morphology of the Au(111) substrate, on the ordered structures, the electrode potential was changed step-by-step and STM images were recorded. The row structure and the Au(111) reconstruction were observed as shown in Figure 1A, even as the electrode potential was stepped as high as 0.55 V_{SCE}. However, when the electrode potential was stepped to 0.65 V_{SCE}, the reconstruction was lifted. The characteristic double stripe structure of the reconstructed Au(111) disappeared, and characteristic monatomic high Au islands, resulting from the lifting of the reconstruction at positive potential,[34] appeared as seen in Figure 2A and B.

At the same time as the reconstruction was lifted, the ordered hexadecane layers disappeared, and rings, about 1 nm in diameter, appeared on the surface. These rings are depressions 0.3−0.5 Å deep. They are present on the terrace and the Au islands. We attribute these rings to hexadecane molecules adopting vertical or tilted orientations. Hexadecane molecules lying flat on the surface enhance tunneling, as evidenced by the imaging of the 2.2 nm long rods as protrusions in the STM images. The enhancement of tunneling of physisorbed insulating molecules has been rationalized by the weak coupling between states in the adsorbate and states in the substrate near the Fermi level.[38] The coupling of these states, which obviously requires geometric proximity, renders the adsorbate an antenna to receive tunneling electrons.[38] The flat orientation of hexadecane molecules allows maximum coupling to the substrate and therefore enhances tunneling. However, if the hexadecane molecules adopt another orientation, e.g., vertical or tilted, in which only a small part of the chain is in van der Waals contact with the substrate, coupling between the molecules and the substrate may be significantly weakened. Tunneling through the molecules may be suppressed to the extent that the tunneling probability through nearby solvent molecules is greater, reversing the contrast. Consequently, the molecules may be imaged in STM as depressions on the surface. Therefore, we speculate that the dark ring structures, enclosing a bright core, are Au clusters surrounded by hexadecane molecules. The density of the rings

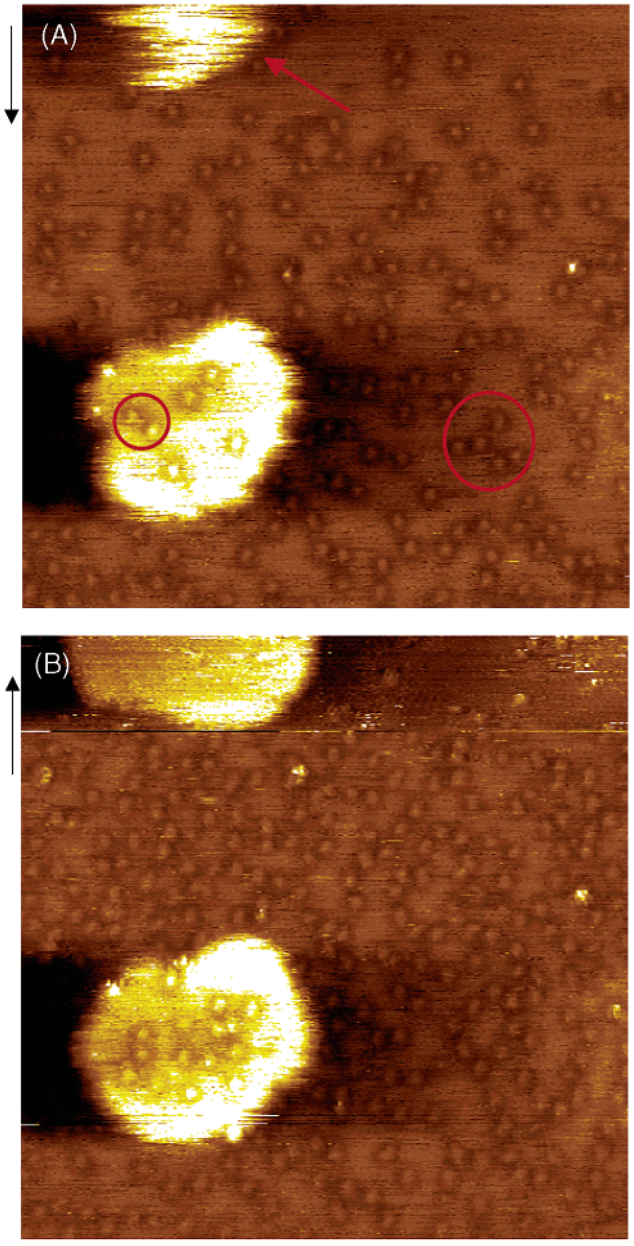

Figure 2. Hexadecane on Au(111) in 0.1 M $HClO_4$ solution at 0.65 V_{SCE}. The reconstruction is lifted and Au islands appear. At the same time, ordered hexadecane rows have disappeared, and dots, about 1 nm in diameter appeared on the surface and grew in number with time. (A) 0−95 s after potential step to 0.65 V_{SCE}, (B) 96−190 s after potential step. Scan area: 32 × 32 nm^2. Scan direction is indicated by black arrows at the top left side of each image.

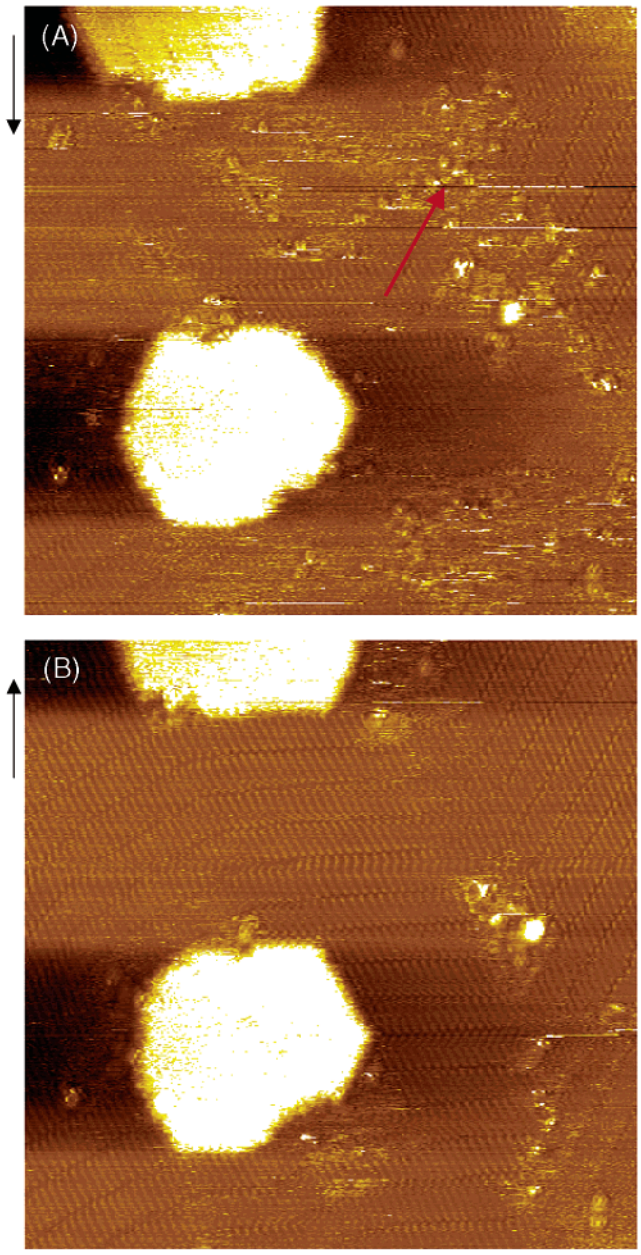

Figure 3. Hexadecane on Au(111) in 0.1 M $HClO_4$ solution at 0.25 V_{SCE} after potential was stepped back from 0.65 V_{SCE}. The dots begin to disappear and the ordered molecular row structures recover on the unreconstructed Au(111) surface. (A) 0−95 s after potential step to 0.25 V_{SCE}, (B) 96−190 s after potential step. Scan area: 32 × 32 nm^2.

increased with time after the lifting of the reconstruction from less than 20/100 nm^2 to about 50/100 nm^2 after 95 s.

The Au islands grew slowly, adopting hexagonal shapes, and their edges became more well-defined, as shown in Figure 2A and Figure 2B, as a function of time. This result differs from our previous studies of the growth and dissolution of nanoscale Au islands in pure 0.1 M $HClO_4$ solutions, where the Au islands created by the lifting of the Au(111) reconstruction formed almost immediately and adopted a shape that was more circular than polygonal.[32] Closer inspection of the images reveals that the island edges are fuzzy, suggesting that the islands are in the process of dynamic evolution.[39] Atoms are continuously attaching, detaching, or diffusing along the island edges. Clearly the presence of the hexadecane molecules affects the structures and dynamics of the gold islands. Au adatoms are ejected onto the surface upon lifting of the reconstruction. The growth of Au islands is a consequence of the aggregation of the adatoms. We suggest that the adsorption of alkanes hinders the surface diffusion of these adatoms, which is necessary for their incorporation into islands, slowing down the growth of the islands. In pure 0.1 M $HClO_4$ solutions, the Au(111) reconstruction lifts at a significantly lower potential, 0.4−0.45 V_{SCE}.[34,36] The STM results presented here suggest that the 2D molecular crystals stabilize the reconstructed herringbone structure of the reconstructed Au(111) to a higher potential than in neat $HClO_4$.

When the potential was stepped back from 0.65 V_{SCE} to 0.25 V_{SCE}, the ring structures disappeared and small clusters, imaged as protrusions, appeared. Simultaneously, the ordered 2D molecular structures recovered on the unreconstructed Au(111) surfaces as shown in Figure 3A. The correlation between the disappearance of the rings and the appearance of ordered

molecular rows suggests that the rings may be composed of aggregated molecules. Therefore, as the alkanes incorporated into the molecular rows, the rings disappeared and the Au clusters left behind are imaged as protrusions. This is consistent with the finding that alkanes form droplets at potentials far away from the pzc but spread out on the metal surface near the pzc.[15] The monatomic high Au islands are observed to assume a hexagonal shape, in sharp contrast to the round shape observed in neat 0.1 M $HClO_4$.[32] This is presumably due to the pinning of the island perimeter atoms by hexadecane molecules. Monatomic Au islands of similar shape have been reported by Lipkowski et al. in their STM study of surfactants adsorbed on Au.[12]

At the potential of 0.65 V_{SCE}, the surface is positively charged, attracting the polar aqueous solvent that presumably displaces the nonpolar hexadecane molecules. Hexadecane is insoluble in water. Hence the adsorbed hexadecane begins to aggregate to minimize hydrophobic interactions. In the SPM study of the potential-dependent structure of dodecyl sulfate on Au(111), Lipkowski. et al. observed that dodecyl sulfate forms hemimicelles near the pzc but desorbs at negative potential.[12] Unlike surfactant molecules, which are soluble in water, the hexadecane molecules cannot leave the surface by desorbing into the bulk aqueous phase. The hexadecane aggregates are probably quite mobile as the area of interaction with the surface is reduced to allow the electrolyte access to the surface, with a concomitant reduction in the binding energy of hexadecane to the surface. However, when the potential was stepped back to 0.25 V_{SCE}, close to the pzc, the aggregated molecules can reassemble into ordered layers to maximize the adsorbate−substrate interaction. This releases the gold atoms trapped in the clusters.

It is worth noting that hexadecane molecules can form ordered structures on an unreconstructed Au(111) surface (Figures 3 and 4). This is in contrast to the result reported in a nonpolar solvent that hexadecane molecules cannot form ordered structures on the unreconstructed Au(111) surface.[28] Comparison with Figure 1 A, acquired before the lifting of reconstruction, allows the determination of the substrate orientations. It can be concluded that the molecular axes are again aligned along nearest neighbor (NN) direction (the $[01\bar{1}]$ or $[1\bar{1}0]$ direction of the unreconstructed Au(111). The similarity of the molecule orientation with respect to lattice on reconstructed (Figure 1A) and unreconstructed (Figure 3B) surfaces suggests that the orientation of the molecular axes in determined by the hexagonal packing of the Au lattice. However, the reconstruction plays a role in pining molecular domain boundaries (Figure 1A).

3.2.2. Order−Disorder Transitions Negative of the pzc. A reversible order−disorder transition is also observed at potentials lower than the pzc. When the electrode potential was stepped from 0.15 V_{SCE} to 0.05 V_{SCE}, the ordered molecular structures disappeared, as shown in Figure 4, indicating that the ordered adlayer transformed into a disordered structure. However, no aggregates, dots, or rings similar to the ones in Figure 2 were observed when the potential induced order−disorder phase transition was triggered. It is assumed that this is due to the lack of Au adatoms, which can only be produced during the lifting of the Au reconstruction at high potentials. These adatoms may be required to form and stabilize the molecule-encapsulated aggregates (rings). The surface becomes more negatively charged as the potential steps from 0.15 V_{SCE} to 0.05 V_{SCE}. (The pzc of unreconstructed Au(111) is about 0.23 V_{SCE}.[34]) The more negative the surface charge, the greater the interaction between the substrate and the polar solvent molecules and

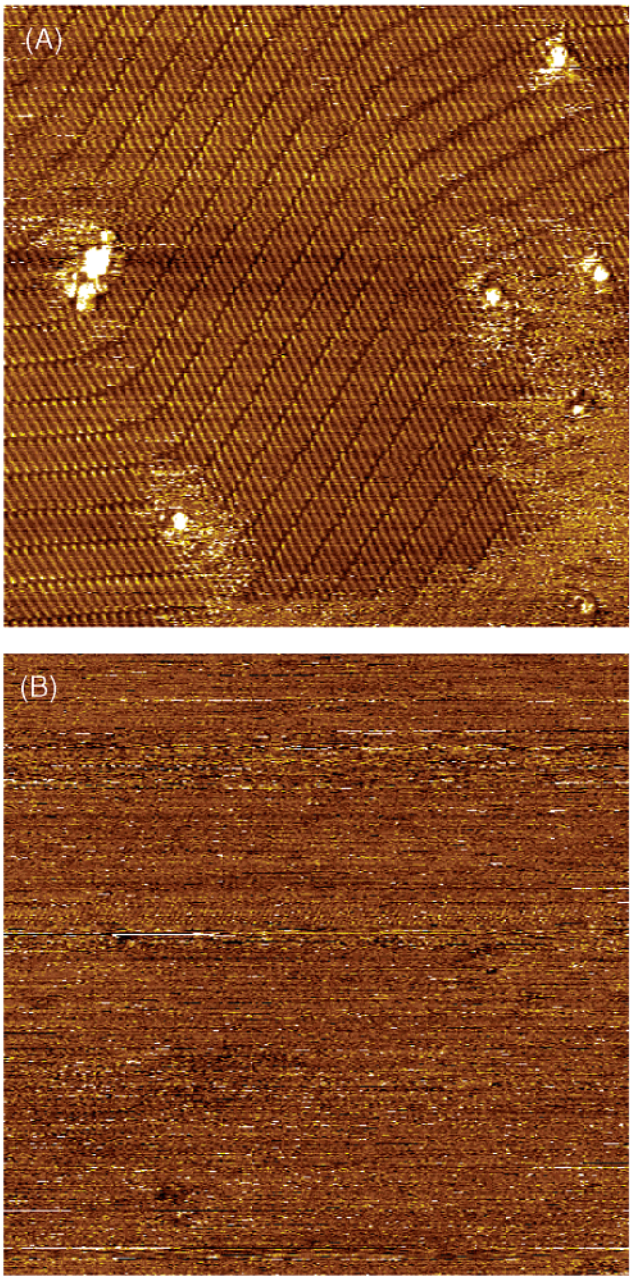

Figure 4. Hexadecane on Au(111) in 0.1 M $HClO_4$ solution. When potential was stepped from 0.15 V_{SCE} (A) to 0.05 V_{SCE} (B), the ordered molecular rows disappeared. Scan area: 32 × 32 nm^2.

positive ions. As a result, the alkane molecules are displaced by the electrolyte at potentials significantly negative of the pzc (Scheme 1).

The potential induced order−disorder transitions are quite reversible. Stepping the potentials back to 0.25 V results in theappearance of ordered molecular domains that initially grew rapidly as evidenced by the almost immediate appearance of molecular rows as shown in Figure 5B. Subsequently, the ordered domain grew slowly at the expense of the disordered domain. The boundary between the ordered and the disordered domains moved along the direction of the ordered molecular rows. It is estimated that the 2D crystal grew at a rate of about 0.2 nm/sec by comparing the position of the domain boundary in Figure 5C with Figure 5B.

We also note that the order−disorder transitions are reversible. This suggests that the molecules displaced by the electrolyte on the charged surface remain in the vicinity of the surface

SCHEME 1: Effect of Surface Charge on Molecular Adsorption[a]

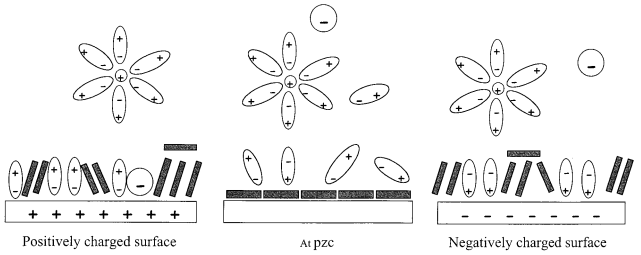

[a] Low surface charge density, hexadecane lies flat, forming an ordered domain. At high surface charge density, solvent is attracted to the substrate, displacing hexadecane on the surface.

instead of being completely desorbed into the electrolyte and diffusing away from the surface (Scheme 1). When the potential returns to the pzc, the displaced molecules are immediately available to form the 2D molecular crystal. This is not surprising considering the hydrophobicity of the hexadecane molecules, manifested by negligible solubility in bulk water.

3.2.3. Spontaneous Molecular Domain Flipping. There are two different possible molecular orientations in a row. In one domain, the molecules are tilted $+60°$ with respect to the molecular rows. In the other they are tilted at $-60°$. The tilt angles are probably related to the symmetry of the Au(111) substrate, indicating the role of adsorbate−substrate interactions in determining the molecular orientation. The presence of two different molecular orientations in a single row is sometimes observed as indicated by arrows in Figure 6A. The boundary between two domains is the line where the molecular 2D crystals show different orientations of molecules in the rows. The images also reveal features that we attribute to the sudden change of molecular orientation that occurs while the image is being acquired. The "partial" molecules observed in Figure 6A are in fact molecules "caught" in the action of changing orientation.

We suggest that the change of molecular orientation is caused by the merging of domains. When two domains merge (Figure 6D), the rows from different domains merge to form a single row, as can be seen in the bottom right-hand corner of Figure 6D. If two rows, each containing molecules with a different orientation, are to merge seamlessly, then the molecules in one of the rows will have to change orientation upon merging so that the new row will contain molecules with a single orientation to minimize repulsion. This reorientation presumably initiates at the domain boundary and travels down the row, a kind of "domino effect", resulting in the observation of "partial" molecules as the reorientation propagates down the row while the STM scans upward. This occurs rapidly as the STM scans because only parts of the flipped molecules are imaged.

The rows indicated by black arrows in Figure 6D have merged, i.e., the molecules in the two rows assume the same orientation. The white arrows in Figure 6D indicate rows that have not yet merged. The domain boundary is noisy, probably reflecting mobile molecules attempting to find the lowest energy configuration. When the merging is complete, molecules in one of the rows must change orientation in order to minimize the repulsion in the new merged row. When two rows containing molecules with different orientations merge, a single orientation ultimately prevails. This indicates the critical role of intermolecular interactions for molecular self-assembly in this system.

The upper limit of the time scale of flipping can be estimated. The clarity of the imaged partial molecules suggests that the flipping of molecules in a row is concerted within the time scale of a scan cycle along the fast axis (~0.1 s). If all the molecules did not flip within a short period of time, the horizontal and tilted molecules would coexist in a row. Due to the stress induced by the molecules with different orientations, the molecules in the row would not be locked in a stable configuration, and would not be clearly imaged by STM. Therefore, the area indicated by arrows in Figure 6A would appear noisy, which it does not. Tip interactions are discounted because (1) the molecules change orientation away from parallel to the fast scanning direction of the tip, the direction one would expect to be favored if tip induced effects were occurring as reported by Stevens et al.,[40] to a direction that makes an angle with the scan direction; (2) further transitions were not observed in subsequent images, although there is still a boundary between the molecular rows with different orientations, and the tip is still interacting with the molecules.

3.2.4. Stabilization of Substrate by Molecular Overlayers. It should be noted that there is no sign of reconstruction of the Au substrate from Figure 3 to Figure 6, even though the substrate is in a potential range where the Au(111) surface should be reconstructed in the absence of adsorbed hexadecane molecules. This indicates that the adsorption of hexadecane stabilizes the unreconstructed Au(111). This is in contrast with the result shown in Figure 2, where the assembled hexadecane molecules stabilize the reconstructed Au(111). The results presented here show that the adsorption of a physisorbed hexadecane stabilizes both the reconstructed structure and unreconstructed structure over a wider potential range than in neat 0.1 M $HClO_4$. In addition to slower diffusion of Au adatoms (discussed in section 3.2.1), another possible reason for the observed stabilization is that the adsorption of insoluble alkane molecules screens the polar H_2O molecules and electrolyte ions from the gold surface, reducing the capacitance and charge density of the double layer. Therefore, in the presence of hexadecane, a more positive potential is required to lift the reconstruction and a more negative potential is required to form reconstruction. As a consequence, both the reconstructed surface and the unreconstructed surface are stable over a wider potential range. It is worth noting the contrasting role in substrate reconstruction played by specifically adsorbed anions, such as Cl^-,[34] that destabilize the reconstruction, shifting the $(1 \times 1) - (22 \times \sqrt{3})$ phase transition potential to more negative values. These anions are believed to facilitate the phase transition between the reconstructed and unreconstructed phase of Au(111) by weakening the bond between the bulk and Au surface atoms.[34] The insoluble hexadecane layer on the contrary probably prevents interactions between the electrolyte and the substrate, until the solvent actually displaces the alkanes.

4. Discussion

The principal interactions that determine the structure of the molecular monolayer at the surface are molecule−substrate interactions and molecule−molecule interactions.[41] If only molecule−solvent interactions were important, one would not expect a strong effect of potential on the observed structures. Physisorbed alkanes interact with the Au surface through weak dispersion forces. In electrochemical systems, one needs to consider the additional effect of surface charge and the electrolyte. Due to the low polarizability of alkanes, any modulation of alkane−substrate interaction by the electric field is expected to be much less than the effect of surface charge in enhancing the adsorption of the aqueous electrolyte. When the electrode potential is at the pzc, the surface is free of charge. It is near this potential that the adsorption of alkane molecules results in the long range ordered structures observed in Figure

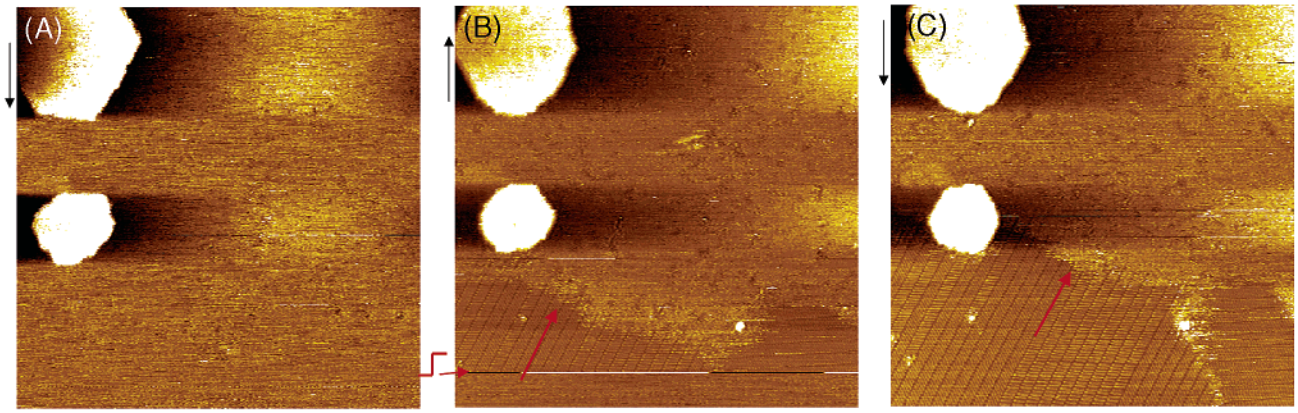

Figure 5. Hexadecane on Au(111) in 0.1 M $HClO_4$ solution (A) obtained at 0.05 V_{SCE}. (B) After potential step to 0.25 V_{SCE}, the ordered molecular rows reappear immediately, and (C) 96−190 s after potential step, ordered molecular layers domain continue to grow. Scan area: 65 × 65 nm^2.

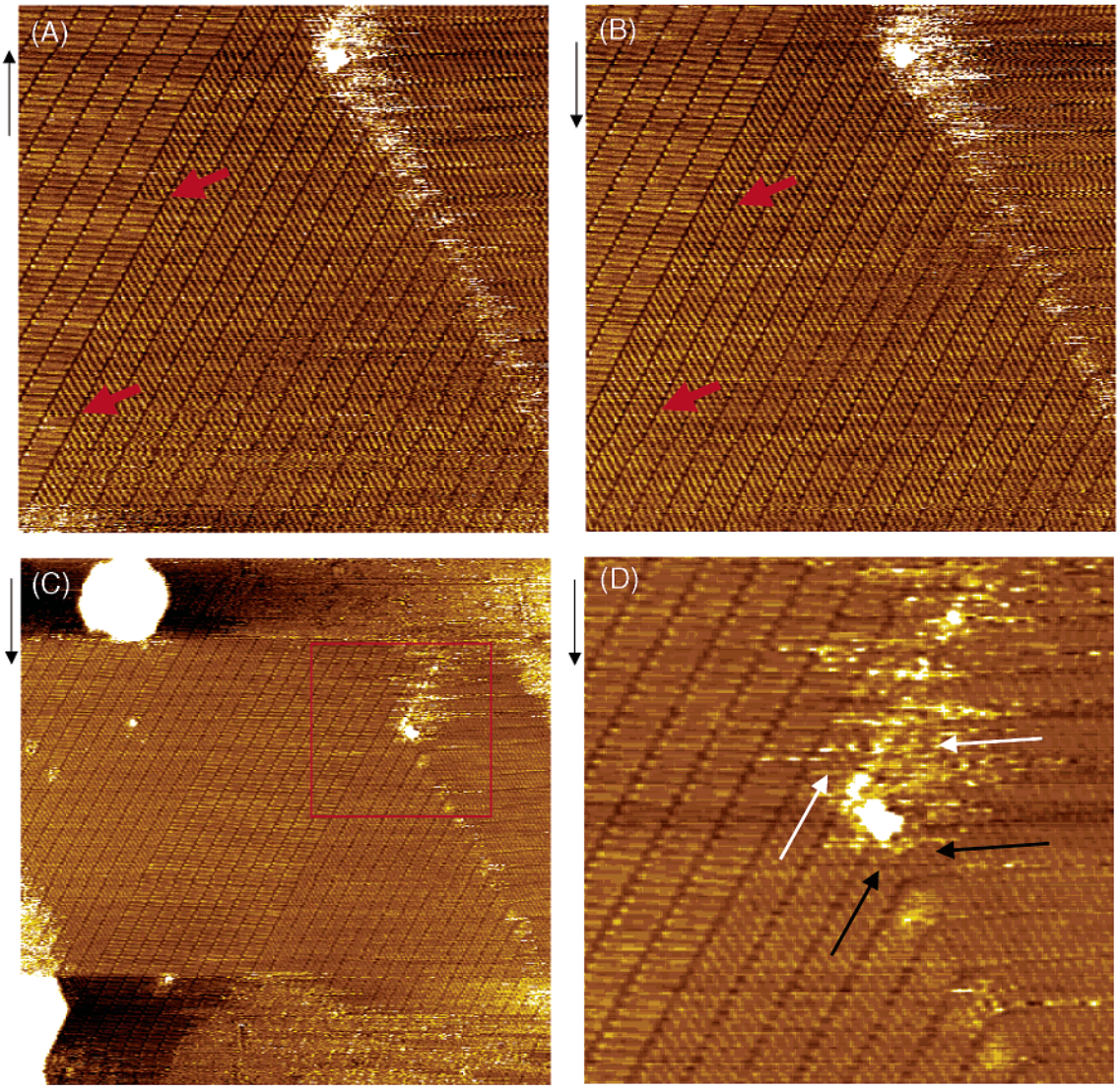

Figure 6. Spontaneous molecular domain flipping: hexadecane on Au(111) in 0.1 M $HClO_4$ solution at 0.25 V_{SCE}. Two different molecular orientations in a single row are indicated by arrows (Figure 6A). A sudden change of molecular orientation during scanning results in a single orientation, Figure 6B. The likely cause is the merging of domains, indicated by arrows in Figure 6D. Scan area (A,B) 34.5 × 34.5 nm^2; (C) obtained before (A), 65 × 65 nm^2; (D) zoom in of Figure 6C, 20 × 20 nm^2.

1. Higher or lower potentials will charge the surface with positive or negative charge, attracting ions and water molecules. This eventually results in the displacement of hexadecane molecules, which leads to the disordering of the adlayer (Scheme 1). However, questions concerning the structure of the displaced hexadecane molecules arise. The rings observed in Figure 2 can be ascribed to alkane aggregates surrounding Au nanoclusters. So far we observed only the ring structures, which we assign to hexadecane containing aggregates, on the surface at positive potential when mobile adatoms are also present due to the lifting

of the reconstruction. It is well known that amphiphilic surfactant molecules can form well-defined aggregates such as hemimicelles at charged interfaces.[3] However, the surfactant hemimicelle aggregates require the presence of hydrophilic headgroups as well as hydrophobic tails.[42] The nature of the interactions that might hold the alkane molecules together in the well-defined nm-sized aggregates is unclear, but is probably driven by hydrophobic effects. We suggest that the aggregates result from the concerted effect of repulsion by aqueous electrolyte and the preferred incorporation of isolated small Au clusters in the core of the aggregate. The nanometer sized Au clusters formed from the lifting of reconstruction may adsorb alkanes more strongly due to the lower coordination number of Au atoms in the clusters. Therefore Au nanoclusters may nucleate and stabilize the presumed alkane aggregates. Despite the high spatial resolution of STM, it is noted that due to the nature of the contrast mechanism, which relies on electron tunneling probabilities, it will probably not be possible to image aggregates adopting conformations characterized by low conductivity, e.g., vertical orientations. Therefore, it will be useful to use AFM to study the structures of alkane aggregates at high surface charge density.

5. Conclusion

This study provides the first direct visualization of potential-dependent structures of adsorbed alkanes at an electrochemical interface. Near the pzc, hexadecane monolayers under electrolyte remarkably resemble those observed under nonpolar solvents in forming ordered monolayers, consisting of molecular rows, on Au surfaces.[25,28] One major difference is the observation of ordered monolayers on unreconstructed Au(111). The structure of molecular adlayers was found to be heavily dependent on electrode potential. Molecular layers at the Au(111) surface can be reversibly switched between ordered and disordered structures by driving the electrode potential away from the pzc. Rings, 1 nm in diameter, were observed when the potential was stepped to 0.65 V on a reconstructed surface previously covered with an ordered hexadecane monolayer. The rings are tentatively assigned to aggregates of hexadecane molecules. When the electrode potential is lower than 0.15 V, the ordered molecular rows disappeared from the negatively charged electrode surface. The ordered molecular rows recovered when the electrode potential returned to voltages close to the pzc of Au(111). The ordered hexadecane rows are observed to stabilize both the reconstructed and unreconstructed Au(111) surfaces. This behavior is assumed to result from the screening of the polar H_2O molecules and electrolyte ions from the gold surface as well as the hindrance of adatom diffusion by adsorbed alkane molecules.

The investigation of alkanes at electrified interfaces may ultimately help to understand and control complex interfacial phenomena such as self-assembly, micelle formation on surfaces, and ion transport through membranes.

Acknowledgment. The authors acknowledge the generous support of the NSF and Research Corporation. E.B. acknowledges the NSF for a CAREER award (CHE-9734273) and the Research Corporation for a Research Innovations Award.

References and Notes

(1) Flink, S.; van Veggel, F. C. J. M.; Reinhoudt, D. N. *Adv. Mater.* **2000**, *12*, 1315.
(2) Laibinis, P. E.; Whitesides, G. M. *J. Am. Chem. Soc.* **1992**, *114*, 9022.
(3) Evans, D. F.; Wennerstrom, H. *The Colloidal Domain: Where Physics, Chemistry, Biology, and Technology Meet*; 2nd ed.; Wiley: New York, 1999.
(4) de Levie, R. *J. Electroanal. Chem.* **1976**, *69*, 265.
(5) Ulman, A. *An Introduction to Ultrathin Organic Films: From Langmuir- Blodgett to Self-Assembly*; Academic Press: Boston, 1991.
(6) Walczak, M. M.; Popenoe, D. D.; Deinhammer, R. S.; Lamp, B. D.; Chung, C.; Porter, M. D. *Langmuir* **1991**, *7*, 2687.
(7) Hatchett, D. W.; Uibel, R. H.; Stevenson, K. J.; Harris, J. M.; White, H. S. *J. Am. Chem. Soc.* **1998**, *120*, 1062.
(8) Kurtyka, B.; de Levie, R. *J. Electroanal. Chem.* **1995**, *397*, 311.
(9) Lipkowski, J.; Stolberg, L. In *Adsorption of Molecules at Metal Electrodes*; Lipkowski, J., Ross, P. N., Eds.; VCH: New York, 1992.
(10) Gao, X. P.; White, H. S.; Chen, S. W.; Abruna, H. D. *Langmuir* **1995**, *11*, 4554.
(11) Bizzotto, D.; Lipkowski, J. *J. Electroanal. Chem.* **1996**, *409*, 33.
(12) Burgess, I.; Jeffrey, C. A.; Cai, X.; Szymanski, G.; Galus, Z.; Lipkowski, J. *Langmuir* **1999**, *15*, 2607.
(13) Esplandiu, M. J.; Hagenström, H.; Kolb, D. M. *Langmuir* **2001**, *17*, 828.
(14) Wu, K.; Iedema, M. J.; Cowin, J. P. *Science* **1999**, *286*, 2482.
(15) Ivosevic, N.; Zutic, V.; Tomaic, J. *Langmuir* **1999**, *15*, 7063.
(16) Wetterer, S. M.; Lavrich, D. J.; Cummings, T.; Bernasek, S. L.; Scoles, G. *J. Phys. Chem. B* **1998**, *102*, 9266.
(17) Xia, T.; Landman, U. *Science* **1993**, *261*, 1310.
(18) Wang, J.-C.; Fichthorn, K. A. *Mater. Res. Soc. Symp. Proc.* **1999**, *543*, 63.
(19) Balasubramanian, S.; Klein, M. L.; Siepmann, J. I. *J. Phys. Chem.* **1996**, *100*, 11960.
(20) Bishop, A. R.; Hostetler, M. J.; Girolami, G. S.; Nuzzo, R. G. *J. Am. Chem. Soc.* **1998**, *120*, 3305.
(21) Yamamoto, M.; Sakurai, Y.; Hosoi, Y.; Ishii, H.; Kajikawa, K.; Ouchi, Y.; Seki, K. *J. Phys. Chem. B* **2000**, *104*, 7363.
(22) Yamamoto, M.; Sakurai, Y.; Hosoi, Y.; Ishii, H.; Ito, E.; Kajikawa, K.; Ouchi, Y.; Seki, K. *Surf. Sci.* **1999**, *428*, 388.
(23) Firment, L. E.; Somorjai, G. A. *J. Chem. Phys.* **1977**, *66*, 2901.
(24) Cyr, D. M.; Venkataraman, B.; Flynn, G. W. *Chem. Mater.* **1996**, *8*, 1600.
(25) Uosaki, K.; Yamada, R. *J. Am. Chem. Soc.* **1999**, *121*, 4090.
(26) Yamada, R.; Uosaki, K. *J. Phys. Chem. B* **2000**, *104*, 6021.
(27) Yamada, R.; Uosaki, K. *Langmuir* **2000**, *16*, 4413.
(28) Xie, Z. X.; Xu, X.; Tang, J.; Mao, B. W. *J. Phys. Chem. B* **2000**, *104*, 11719.
(29) Xie, Z. X.; Xu, X.; Tang, J.; Mao, B. W. *Chem. Phys. Lett.* **2000**, *323*, 209.
(30) Marchenko, O.; Cousty, J. *Phys. Rev. Lett.* **2000**, *84*, 5363.
(31) Marchenko, A.; Xie, Z. X.; Cousty, J.; Van, L. P. *Surf. Interface Anal.* **2000**, *30*, 167.
(32) He, Y.; Borguet, E. *J. Phys. Chem. B* **2001**, *105*, 3981.
(33) Whitton, J. L.; Davies, J. A. *J. Electrochem. Soc.* **1964**, *111*, 1347.
(34) Kolb, D. M. *Prog. Surf. Sci.* **1996**, *51*, 109.
(35) Gao, X.; Hamelin, A.; Weaver, M. J. *J. Chem. Phys.* **1991**, *95*, 6993.
(36) Tao, N. J.; Lindsay, S. M. *Surf. Sci.* **1992**, *274*, L546.
(37) Hentschke, R.; Schürmann, B. L.; Rabe, J. P. *J. Chem. Phys.* **1992**, *96*, 6213.
(38) Giancarlo, L. C.; Flynn, G. W. *Annu. Rev. Phys. Chem.* **1998**, *49*, 297.
(39) Giesen, M.; Dietterle, M.; Stapel, D.; Ibach, H.; Kolb, D. M. *Surf. Sci.* **1997**, *384*, 168.
(40) Stevens, F.; Buehner, D.; Beebe, T. P. *J. Phys. Chem. B* **1997**, *101*, 6491.
(41) Van Hove, M. A. In *Structure of Electrified Interfaces*; Lipkowski, J., Ross, P. N., Eds.; VCH: New York, 1993.
(42) Nagarajan, R. *Langmuir* **2002**, *18*, 31.